Nanoscale

RSC Publishing

PAPER

View Article Online
View Journal | View Issue

Ratiometric fluorescent nanosensor based on water soluble carbon nanodots with multiple sensing capacities†

Cite this: *Nanoscale*, 2013, **5**, 5514

Songnan Qu, Hong Chen, Xuanming Zheng, Junsheng Cao and Xingyuan Liu*

A construction strategy for ratiometric fluorescent nanosensors based on water soluble C-dots was developed, which could sense temperature (10–82 °C), pH values (lower than 6.0 or higher than 8.6) and Fe^{3+} ions (>0.04 μM) by monitoring the intensity ratios of dual fluorescence bands (I_b/I_g) under 380 nm excitation. I_b/I_g decreased nearly linearly with increasing temperature from 10 to 82 °C. In the pH range from 8.6 to 6.0, the I_b/I_g was nearly constant at 0.75. I_b/I_g gradually decreased from 0.75 to 0.52 in the pH range from 6.0 to 1.9, and increased nearly linearly from 0.52 to 0.75 in the pH range from 1.9 to 1.0. The dual fluorescence behavior was reversible in the pH range from 1.0 to 8.6. As pH increased from 10.6 to 13.0, the green fluorescence band decreased continuously and blue shifted with a nearly linear increase in I_b/I_g from 0.75 to 2.15, while the green fluorescence band cannot be recovered by decreasing the pH value. I_b/I_g was ultrasensitive and selective in presence of Fe^{3+} (>0.04 μM) in neutral aqueous environments. The two fluorescence bands of the C-dots were attributed to different surface states that may produce different fluorescent signal responses to external physical or chemical stimuli.

Received 3rd February 2013
Accepted 31st March 2013

DOI: 10.1039/c3nr00619k

www.rsc.org/nanoscale

Introduction

Fluorescent carbon nanodots (C-dots) are newly emerging as versatile fluorescent nanomaterials with many potential applications.[1] Compared to organic dyes and semiconductor quantum dots with heavy metal cores, C-dots are superior in terms of chemical inertness, their lack of optical blinking, low photobleaching, low cytotoxicity, biocompatibility, water solubility, and tunable excitation and emission spectra. Therefore, C-dots are promising as substitutes for organic dyes or semiconductor quantum dots with heavy metal cores for preparation of fluorescent nanosensors, and have attracted considerable attention.

C-dot based fluorescent nanosensors have been undergoing rapid development recently. By monitoring the changes in their fluorescence intensity under external physical or chemical stimuli, C-dots have been used to detect substances and quantities such as DNA,[2] PO_4^{3-},[3] lysozyme,[4] thrombin,[5] nitrite,[6] glucose,[7] biothiol,[8] pH,[9] Ag^+,[10] Hg^{2+},[11] and Cu^{2+}.[12] However, most of these C-dot based fluorescent nanosensors are based on single wavelength fluorescence intensity change methods. Fluorescence intensity-based methods circumvent many problems, such as signal variations caused by fluctuations in concentration, optical path length and source intensity, which otherwise prevent precise and quantitative determination. Ratiometric fluorescent sensors, which use the intensity ratio of two well-resolved wavelengths, and thus provide built-in correction for environmental interference, could improve the quantification accuracy, and therefore have great advantages over single wavelength fluorescent change probes.[13] Ratiometric fluorescent sensors are usually used in dual excitation mode, which has some drawbacks, such as complex equipment and operation and poor time resolution. The design and development of ratiometric fluorescent nanosensors based on C-dots in single excitation mode are attracting great interest, particularly in the intracellular sensing field. Ma *et al.* developed a ratiometric fluorescent pH nanosensor by incorporating fluorescein isothiocyanate (FITC) and rhodamine B isothiocyanate (RBITC) with C-dots, which enabled the intracellular pH pattern of HeLa cells to be quantitatively obtained under 488 nm excitation.[14] Zeng *et al.* developed a ratiometric fluorescent nanosensor by incorporating a naphthalimide azide derivative with C-dots for detecting H_2S in aqueous media and serum, as well as inside live cells under 340 nm excitation.[15] Tian *et al.* reported a ratiometric fluorescent nanosensor based on C-dot hybridized CdSe/ZnS quantum dots that could selectively and sensitively sense and image Cu^{2+} ions intracellularly under 400 nm

State Key Laboratory of Luminescence and Applications, Changchun Institute of Optics, Fine Mechanics and Physics, Chinese Academy of Sciences, Changchun, 130033, P. R. China. E-mail: liuxy@ciomp.ac.cn; Songnanqu@yahoo.cn; Tel: +86 431 86176341

† Electronic supplementary information (ESI) available: Experimental details, PL spectra of the C-dots in different media and conditions. See DOI: 10.1039/c3nr00619k

excitation.[16] However, these methods inevitably brought in the drawbacks of organic dyes or semiconductor quantum dots with heavy metal cores, and weakened the merits of C-dots.

In our recent work, we reported a simple, economical and green single-step microwave synthesis method for water-soluble luminescent C-dots for application to a new type of biocompatible fluorescent ink.[17] These C-dots display zero or low toxicity to both plants and animals, and showed stable, excitation-wavelength-dependent photoluminescence (PL) properties in aqueous solutions. Here, we report the multiple sensing capacities of these C-dots on the basis of ratiometric fluorescence. To the best of our knowledge, this is the first ratiometric fluorescent nanosensor based on C-dots without incorporation of organic dyes or hybridization of semiconductor quantum dots with heavy metal cores.

Results

Excitation and fluorescence lifetime decay spectra investigations

The synthesis process for these C-dots can be found in our previous work.[17] Under single wavelength excitation at 380 nm, the C-dot dilute aqueous solutions showed two well resolved fluorescent bands centered at 455 and 520 nm (Fig. 1a). The PL excitation spectra of the C-dot dilute aqueous solution recorded at 455 and 520 nm showed two different π–π^* transition bands centered at 357 and 408 nm, respectively. The fluorescent decay curves of the C-dot aqueous solution recorded at 455 and 520 nm under excitation at 380 nm produced different fluorescent lifetimes (Fig. 1b). The average fluorescence lifetimes recorded at 455 nm and 520 nm were 9.5 ns and 6.5 ns, respectively. These results indicated that the two well resolved blue and green fluorescence bands under 380 nm excitation were from different electronic transition processes, which might produce different fluorescent signal responses to external physical or chemical stimuli. After 3 h of continuous excitation at 380 nm (light source: 450 W Xe lamp, excitation slit: 1 nm), the two fluorescence bands showed fewer fluctuations and the intensity ratio of the two bands was nearly constant under the same test conditions (Fig. S1†), showing that C-dots could be used as ratiometric fluorescent nanosensors on the basis of this dual fluorescence.

Temperature sensing capacity

The effects of temperature on the two fluorescence bands of the C-dot aqueous solutions (excitation at 380 nm) were investigated (Fig. 2a and b). In the range from 10 to 82 °C, the blue band gradually decreased while the green band increased slightly (Fig. S2†). The intensity ratio of the two fluorescence bands (I_b/I_g) decreased nearly linearly with increasing temperature. Under decreasing temperature, the dual fluorescence behavior of the C-dot aqueous solutions was reversible, indicating a ratiometric fluorescent sensing capacity for temperature.

pH sensing capacity

Detection of pH is critically important because it plays a pivotal role in many systems. In contrast to most common pH probes based on electrochemical methods, fluorescence-based pH nanosensors have distinct advantages in intracellular pH and microscopy studies.[9,14,18] The pH sensing capacity of the C-dot dilute aqueous solution was studied for a wide range of pH values (which were adjusted by adding HCl or NaOH) under 380 nm excitation at 25 °C (Fig. 3a and b). In the pH range from 8.6 to 6.0, the two fluorescence bands showed small fluctuations, and I_b/I_g was nearly constant at 0.75. For decreasing pH values from 6.0 to 1.9, both fluorescence bands decreased obviously (Fig. S3a†), and I_b/I_g decreased gradually from 0.75 to 0.52. For decreasing pH values from 1.9 to 1.0, the blue fluorescence band decreased further, while the green fluorescence band decreased greatly and blue shifted (Fig. 3c and d). I_b/I_g increased nearly linearly from 0.52 to 0.75 for the pH values from 1.9 to 1.0. For increasing pH values from 1.0 to 8.6 by addition of NaOH, the dual fluorescence behavior was seen to be reversible. For increasing pH values from 8.6 to 13.0, the blue fluorescence band first slightly increased and then decreased, while the green fluorescence band continuously decreased and blue shifted (Fig. S3b†). I_b/I_g increased nearly linearly from 0.82 to 1.36 for pH values from 10.6 to 13.0. However, the green fluorescence band cannot be recovered by adding HCl to neutral aqueous solution (Fig. S4†). This indicates that the C-dots can be used as ratiometric fluorescent pH nanosensors at pH values lower than 6.0 or higher than 8.6.

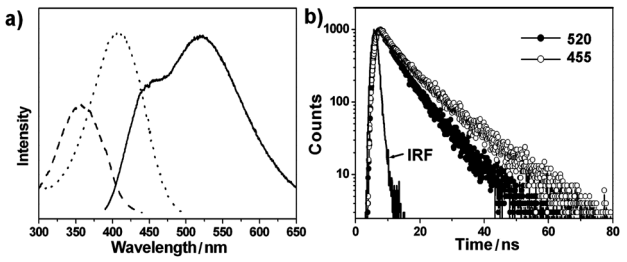

Fig. 1 (a) Fluorescence excitation and fluorescence emission spectra of a C-dot dilute aqueous solution at 25 °C (emission wavelengths for excitation spectra: 455 nm (dashed line) and 520 nm (dotted line), excitation wavelength for emission spectrum: 380 nm). (b) Fluorescence decay at 455 nm and 520 nm of the C-dot dilute aqueous solution at 25 °C (excitation at 380 nm; IRF = instrument response function).

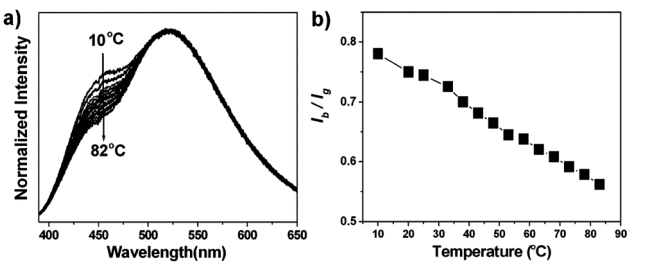

Fig. 2 (a) PL spectra of the C-dot dilute aqueous solution (0.1 mg mL^{-1}) at different temperatures (normalized at the maximum peak of the green fluorescence band, 380 nm excitation). (b) Plots of I_b/I_g *versus* temperature.

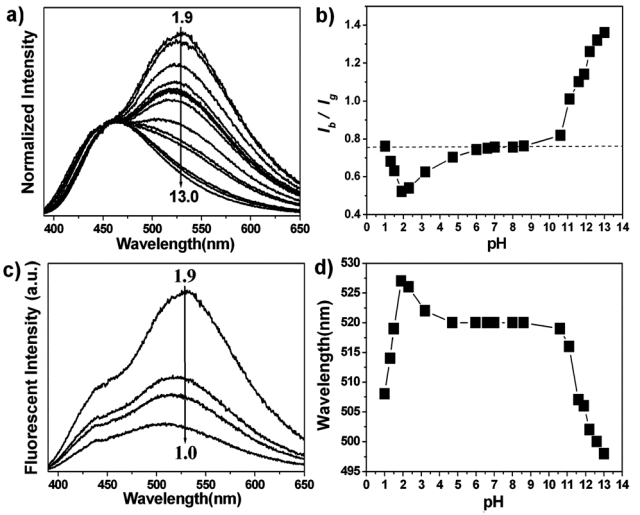

Fig. 3 (a) PL spectra of the C-dot aqueous solutions (0.1 mg mL^{-1}) for pH values from 1.9 to 13.0 (normalized at the maximum peak of the blue fluorescence band, 380 nm excitation, at 25 °C). (b) Plots of I_b/I_g *versus* pH. (c) PL spectra of the C-dot aqueous solutions (0.1 mg mL^{-1}) for pH values from 1.9 to 1.0 (380 nm excitation at 25 °C). (d) Plots of the wavelengths of the maximum peaks of the green fluorescence bands *versus* pH.

Metal ions sensing capacity

Detection of transition metal ions at the micromolar level is highly desirable because of the vital roles they play in biological and environmental applications.[19] Fe^{3+} is an important transition metal for all organisms, and disorders in its metabolism cause anemia, liver and kidney damage, diabetes, and heart failure.[20] However, many Fe^{3+}-selective fluorescent sensors are hydrophobic, and this incompatibility with aqueous environments restricts the application of these sensors in biological systems.[21] Zhou *et al.* reported a pyrene-bearing cellulose nanocrystals that could selectively and sensitively sense Fe^{3+} ions at concentrations higher than 1 μM in aqueous suspension based on single wavelength fluorescence intensity change method.[22] Kumar *et al.* reported a thiacalix[4]arene based fluorescent probe for sensing and imaging of Fe^{3+} ions in aqueous media based on single wavelength fluorescence intensity change method with the detection limit of about 0.5 μM.[23] Ratiometric fluorescent nanosensors for Fe^{3+} are scarce in aqueous environments. Thennarasu *et al.* reported a single molecular FRET based sensor for ratiometric detection of Fe^{3+} ions in aqueous media with the detection limit of about 0.05 μM.[24] As demonstrated above, I_b/I_g of the C-dot aqueous solution was nearly constant in the pH range from 8.6 to 6.0 at 25 °C, indicating potential metal ions sensing applications in physiological samples. The dual fluorescence responses of the C-dot aqueous solution (380 nm excitation) to Fe^{3+} ions ($Fe(NO_3)_3$) were measured in the pH range from 8.6 to 6.0 at 25 °C. Upon addition of Fe^{3+} ions, as shown in Fig. S5,† the green fluorescence band gradually decreased and red shifted slightly, while the blue fluorescence band was dramatically quenched. The dual fluorescence of the C-dot aqueous solution is sensitive to the detection of Fe^{3+} ions at concentrations above 0.04 μM. As the Fe^{3+} ion concentration increased from 0.04 to 46 μM, I_b/I_g gradually decreased from 0.73 to 0.49 (Fig. 4c and d). The time-dependent PL spectra of a C-dot–Fe^{3+} solution shown in Fig. S6† indicate that only 1 min is required to complete the reaction between the C-dots and Fe^{3+}. To evaluate the selectivity of the sensing system, we measured I_b/I_g in the presence of various metal ions under the same conditions, including Ca^{2+}, Cd^{2+}, Cu^{2+}, Ba^{2+}, Al^{3+}, Na^{+}, Mg^{2+}, Ni^{2+}, Pb^{2+}, Zn^{2+} and Ag^{+}, as shown in Fig. 4b. No obvious changes in I_b/I_g were observed for most of these metal ions in the same measuring condition. It was found that Cu^{2+} could also quench the dual fluorescence of the C-dot aqueous solution with a decreased I_b/I_g. Further experiments showed that the dual fluorescence of the C-dot aqueous solution was sensitive to Cu^{2+} ions at concentrations higher than 30 μM (Fig. 4d and S7†). As the Cu^{2+} ion concentration increased from 30 to 480 μM, I_b/I_g gradually decreased from 0.73 to 0.62, indicating that the amount of Cu^{2+}, at more than 500 times that of Fe^{3+}, interfered with the detection of Fe^{3+}. As the method has a higher sensitivity to Fe^{3+} than to Cu^{2+} and I_b/I_g cannot be found at less than 0.62 in presence of Cu^{2+} at concentration low than 480 μM, the interference from Cu^{2+} could be eliminated by simply diluting the sample. Overall, these observations indicate that the C-dots can be used as ratiometric fluorescent nanosensors for ultrasensitive and selective detection of Fe^{3+} in aqueous environmental and biological systems.

To evaluate the C-dot based Fe^{3+} sensor in an artificial system, the performance of the present method for real water sample analysis was challenged by lake water samples obtained from the South Lake of Changchun, Jilin province, China. The lake water samples were filtered through a 0.22 μm membrane and then centrifuged at 15 000 rpm for 20 min. The resultant

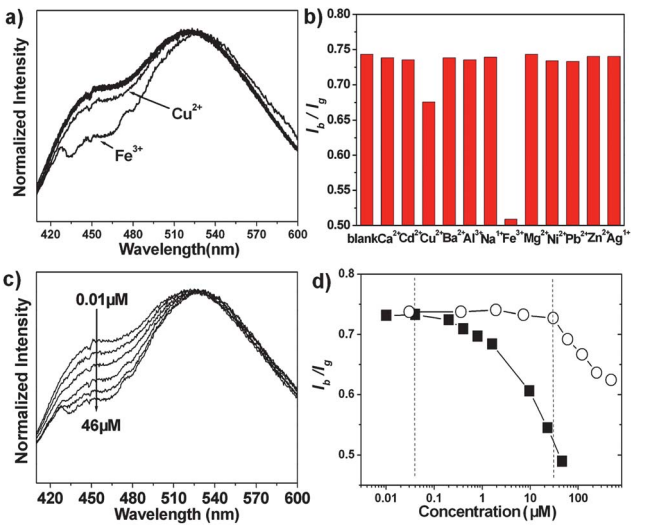

Fig. 4 (a) PL spectra of the C-dot aqueous solutions (0.02 mg mL^{-1}) in the absence and presence of different metal ions (normalized at the maximum peak of the green fluorescence band, 380 nm excitation at 25 °C, 50 μM of selected metal ions). (b) I_b/I_g of the C-dot aqueous solutions (0.02 mg mL^{-1}) in the absence and the presence of different metal ions (380 nm excitation at 25 °C, 50 μM of selected metal ions). (c) PL spectra of the C-dot aqueous solutions (0.02 mg mL^{-1}) in the presence of different Fe^{3+} concentrations (normalized at the maximum peak of the green fluorescence band, 380 nm excitation at 25 °C). (d) Plots of I_b/I_g *versus* Fe^{3+} (■) and Cu^{2+} (○) concentrations.

water samples were spiked with Fe^{3+} at different concentration levels and then analyzed with the proposed method. It is seen that the PL intensity and I_b/I_g gradually decreased with increasing the concentration of Fe^{3+} from 0.6 to 80 μM, as shown in Fig. S8.† In spite of the interference from numerous minerals and organics existing in lake water, this sensing platform can still distinguish between fresh lake water and that spiked with Fe^{3+} at concentrations higher than 0.6 μM. These results imply that the Fe^{3+} sensor is likely to be capable of practically useful Fe^{3+} detection upon further development.

Discussions

It has been shown that the surface state and size may affect the emission of C-dots.[1] At present, the mechanism of the multiple sensing capacities of the C-dots is unclear. We proposed that the dual fluorescent bands of the C-dots could be attributed to different surface states. The Fourier transform IR (FTIR) spectrum revealed that the C-dots contained N–H and C=O, which was attributed to urea groups on the surface.[17] Adjacent urea groups on the C-dots could form intramolecular H-bonds, which may lead to extended conjugation in the structure of the C-dots. These intramolecular H-bonds could be destroyed by the surrounding polar solvent molecules and form intermolecular H-bonds between the urea groups and the solvent molecules. The urea group is non-fluorescent group. Intramolecular H-bonding or intermolecular H-bonding urea groups might lead to different surface states of the C-dots. We proposed the blue fluorescence band was attributed to a surface state in which urea groups formed intermolecular H-bonds, while the green fluorescence band was attributed to a surface state in which urea groups formed intramolecular H-bonds, as shown in Scheme 1. The intermolecular H-bonds are more sensitive to temperature than the intramolecular H-bonds.[25] At high temperatures, intermolecular H-bonds between the urea groups and water molecules are greatly weakened, and the urea groups tend to form intramolecular H-bonds, which might explain the decrease in I_b/I_g with increasing temperature. In the pH range from 6.0 to 1.9, the decrease of the two fluorescence bands may be caused by protonation of the urea groups. The intermolecular H-bonding urea groups are easier to contact with hydrogen ions than the intramolecular H-bonding urea groups. The protonation process of the intermolecular H-bonding urea groups is faster than that of intramolecular H-bonding urea groups, which may explain the gradual decrease in I_b/I_g in the pH range from 6.0 to 1.9. At pH values lower than 1.9, protonation of the intermolecular H-bonding urea groups was nearly complete, and further protonation of intramolecular H-bonding urea groups occurred, which may be the reason for the near-linear increase in I_b/I_g in the pH range from 1.9 to 1.0. The reversible dual fluorescence behavior in the pH range from 1.0 to 8.6 can be understood in terms of deprotonation of the urea groups. For pH values higher than 8.6, intramolecular H-bonds between the urea groups were gradually destroyed by increased hydroxyl ions. In strong alkaline aqueous environments (pH >10.5), the urea groups were gradually hydrolyzed, and intramolecular H-bonding urea groups diminished greatly, which may be the reason for the irreversible decrease and blue shifted green fluorescence band in the pH range from 10.6 to 13.0. N–H group is known for strong binding affinity to transition and post-transition metals. The intermolecular H-bonding urea groups have more free N–H groups than intramolecular H-bonding urea groups. It might be the case that intermolecular H-bonding urea groups are the primary bonding sites on the C-dots with metal ions, which may explain the faster attenuation of the blue fluorescence band compared to the green fluorescence band upon addition of Fe^{3+} ions. The quenching caused by complexation of Fe^{3+} ions is most likely due to the electron/energy transfer process occurring between the excited C-dots and the redox active metal ions. In our recent work, the green fluorescence band was greatly increased in dry states,[17] which may support our proposal that no solvent molecule interfered with urea groups in the formation of intramolecular H-bonds on the C-dot surfaces and led to the enhanced green fluorescence band. We also speculate that the C-dot size and the urea group density on the surface of the C-dots can also affect urea groups in the formation of intramolecular H-bonds. Further studies are in progress.

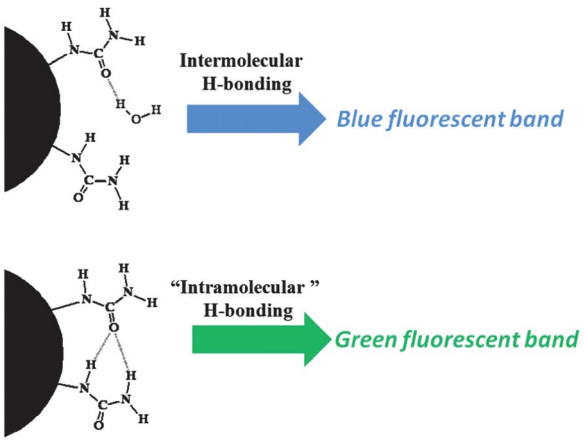

Scheme 1 Schematic representation of two possible surface states of the C-dots for dual fluorescence bands.

Conclusions

In conclusion, we have developed ratiometric fluorescent nanosensors based on water soluble C-dots for precise and quantitative sensing of temperature, pH values and Fe^{3+} ions by monitoring the intensity ratios of the dual fluorescence bands (I_b/I_g) under 380 nm excitation. I_b/I_g decreased nearly linearly with increasing temperature from 10 to 82 °C. I_b/I_g gradually decreased from 0.75 to 0.52 in the pH range from 6.0 to 1.9, and increased nearly linearly from 0.52 to 0.75 in the pH range from 1.9 to 1.0. The dual fluorescence behavior was reversible in the pH range from 1.0 to 8.6. As pH increased from 10.6 to 13.0, the green fluorescence band decreased continuously and blue shifted with a nearly linear increase in I_b/I_g from 0.75 to 2.15, while the green fluorescence band cannot be recovered by decreasing the pH value. I_b/I_g was ultrasensitive and selective in presence of Fe^{3+} (>0.04 μM) in neutral aqueous environments. With increasing Fe^{3+} ion concentration from 0.04 to 50 μM, I_b/I_g

gradually decreased from 0.73 to 0.49. The two fluorescence bands of the C-dots were attributed to different surface states that may produce different fluorescent signal responses to external physical or chemical stimuli. Further studies of the mechanism of the C-dot sensing capacities and the C-dot intracellular sensing behaviors are in progress. This work provides a promising method for construction of ratiometric fluorescent nanosensors based on C-dots with various sensing capacities.

Acknowledgements

This work is supported by the CAS Innovation Program, the Jilin Province Science and Technology Research Project through Grant no. 201101080, and the National Science Foundation of China through Grant no. 51103144, 51102228, 61106057 and 61274126.

Notes and references

1 (*a*) S. N. Baker and G. A. Baker, *Angew. Chem., Int. Ed.*, 2010, **49**, 6726; (*b*) J. C. G. Esteves da Silva and H. M. R. Goncalves, *TrAC, Trends Anal. Chem.*, 2011, **30**, 1327; (*c*) H. Li, Z. Kang, Y. Liu and S. T. Lee, *J. Mater. Chem.*, 2012, **22**, 24230.

2 (*a*) W. J. Bai, H. Z. Zheng, Y. J. Long, X. J. Mao, M. Gao and L. Y. Zhang, *Anal. Sci.*, 2011, **27**, 243; (*b*) H. L. Li, Y. W. Zhang, L. Wang, J. Q. Tian and X. P. Sun, *Chem. Commun.*, 2011, **47**, 961.

3 H. X. Zhao, L. Q. Liu, Z. D. Liu, Y. Wang, X. J. Zhao and C. Z. Huang, *Chem. Commun.*, 2011, **47**, 2604.

4 L. Q. Liu and Y. F. Li, *J. Southwest Univ., Nat. Sci. Ed.*, 2010, **32**, 25.

5 J. H. Liu, J. S. Li, Y. Jiang, S. Yang, W. H. Tan and R. H. Yang, *Chem. Commun.*, 2011, **47**, 11321.

6 Z. Lin, W. Xue, H. Chen and J. M. Lin, *Anal. Chem.*, 2011, **83**, 8245.

7 W. B. Shi, Q. L. Wang, Y. J. Long, Z. L. Cheng, S. H. Chen, H. Z. Zheng and Y. M. Huang, *Chem. Commun.*, 2011, **47**, 6695.

8 L. Zhou, Y. H. Lin, Z. Z. Huang, J. S. Ren and X. G. Qu, *Chem. Commun.*, 2012, **48**, 1147.

9 (*a*) X. Jia, J. Lia and E. Wang, *Nanoscale*, 2012, **4**, 5572; (*b*) M. J. Krysmann, A. Kelarakis, P. Dallas and E. P. Giannelis, *J. Am. Chem. Soc.*, 2012, **134**, 747.

10 H. L. Li, J. F. Zhai and X. P. Sun, *Langmuir*, 2011, **27**, 4305.

11 H. L. Li, J. F. Zhai, J. Q. Tian, Y. L. Luo and X. P. Sun, *Biosens. Bioelectron.*, 2011, **26**, 4656.

12 (*a*) Q. Qu, A. Zhu, X. Shao, G. Shi and Y. Tian, *Chem. Commun.*, 2012, **48**, 5473; (*b*) J. M. Liu, L. Lin, X. X. Wang, S. L. Lin, W. L. Cai, L. H. Zhang and Z. Y. Zheng, *Analyst*, 2012, **137**, 2637; (*c*) S. Liu, J. Tian, L. Wang, Y. Zhang, X. Qin, Y. Luo, A. M. Asiri, A. O. Al-Youbi and X. Sun, *Adv. Mater.*, 2012, **24**, 2037.

13 K. Zhang, H. Zhou, Q. Mei, S. Wang, G. Guan, R. Liu, J. Zhang and Z. Zhang, *J. Am. Chem. Soc.*, 2011, **133**, 8424.

14 W. Shi, X. Li and H. Ma, *Angew. Chem., Int. Ed.*, 2012, **51**, 6432.

15 C. Yu, X. Li, F. Zeng, F. Zheng and S. Wu, *Chem. Commun.*, 2013, **49**, 403.

16 A. Zhu, Q. Qu, X. Shao, B. Kong and Y. Tian, *Angew. Chem., Int. Ed.*, 2012, **51**, 7185.

17 S. Qu, X. Wang, Q. Lu, X. Liu and L. Wang, *Angew. Chem., Int. Ed.*, 2012, **51**, 12215.

18 (*a*) J. Y. Han and K. Burgess, *Chem. Rev.*, 2010, **110**, 2709; (*b*) T. Myochin, K. Kiyose, K. Hanaoka, H. Kojima, T. Terai and T. Nagano, *J. Am. Chem. Soc.*, 2011, **133**, 3401; (*c*) M. Tantama, Y. P. Hung and G. Yellen, *J. Am. Chem. Soc.*, 2011, **133**, 10034; (*d*) R. V. Benjaminsen, H. Sun, J. R. Henriksen, N. M. Christensen, K. Almdal and T. L. Andresen, *ACS Nano*, 2011, **5**, 5864; (*e*) Y. P. Chen, H. A. Chen, Y. Hung, F. C. Chien, P. Chen and C. Y. Mou, *RSC Adv.*, 2012, **2**, 968; (*f*) M. J. Marin, F. Galindo, P. Thomas and D. A. Russell, *Angew. Chem., Int. Ed.*, 2012, **51**, 9657.

19 (*a*) A. P. de Silva, H. Q. N. Gunaratne, T. Gunnlaugsson, A. J. M. Huxley, C. P. McCoy, J. T. Rademacher and T. E. Rice, *Chem. Rev.*, 1997, **97**, 1515; (*b*) B. Valeur and I. Leray, *Coord. Chem. Rev.*, 2000, **205**, 3.

20 (*a*) C. Brugnara, *Clin. Chem.*, 2003, **49**, 1573; (*b*) X. B. Zhang, G. Cheng, W. J. Zhang, G. Shen and R. Q. Yu, *Talanta*, 2007, **71**, 171.

21 (*a*) Z. Q. Hu, Y. C. Feng, H. Q. Huang, L. Ding, X. M. Wang, C. S. Lin, M. Li and C. P. Ma, *Sens. Actuators, B*, 2011, **156**, 428; (*b*) Z. X. Li, L. F. Zhang, W. Y. Zhao, X. Y. Li, Y. K. Guo, M. M. Yu and J. X. Liu, *Inorg. Chem. Commun.*, 2011, **14**, 1656.

22 L. Zhang, Q. Li, J. Zhou and L. Zhang, *Macromol. Chem. Phys.*, 2012, **213**, 1612.

23 M. Kumar, R. Kumar, V. B. Pa, R. Sharma, T. Kaurb and Y. Qurishi, *Dalton Trans.*, 2012, **41**, 408.

24 N. R. Chereddy, S. Thennarasu and A. B. Mandal, *Analyst*, 2013, **138**, 1334.

25 (*a*) Y. Hamuro, S. J. Geib and A. D. Hamilto, *J. Am. Chem. Soc.*, 1996, **118**, 7529; (*b*) Y. Hamuro, S. J. Geib and A. D. Hamilto, *J. Am. Chem. Soc.*, 1997, **119**, 10587; (*c*) S. Qu, F. Li, H. Wang, B. Bai, C. Xu, L. Zhao, B. Long and M. Li, *Chem. Mater.*, 2007, **19**, 4839.

